

Elastic Properties of 2D amorphous solids

Christian L. Klix,¹ Florian Ebert,¹ Fabian Weysser,¹ Matthias Fuchs,¹ Georg Maret,¹ and Peter Keim¹

¹University of Konstanz, D-78457 Konstanz, Germany

(Dated: November 9, 2011)

Using positional data from video-microscopy of a two-dimensional colloidal system and from simulations of hard discs we determine the wave-vector-dependent normal mode spring constants in the supercooled fluid and glassy state, respectively. The emergence of rigidity and the existence of a displacement field in amorphous solids is clarified. Continuum elastic theory is used in the limit of long wavelengths to analyze the bulk and shear modulus of this amorphous system as a function of temperature. The onset of a finite static shear modulus upon cooling marks the fluid/solid transition. This provides an opportunity to determine the glass transition temperature T_g in an intuitive and precise way.

PACS numbers: 82.70.Dd, 61.20.Ja

In general, there are different ways to characterize supercooled or glassy systems. For instance, a characteristic change in the thermodynamic properties, e.g. volume and enthalpy, upon cooling a fluid may be used to define the glass transition temperature T_g [1]. Another property often investigated for molecular or atomic glasses is the viscosity η . Given the rapid slowing down of the dynamics upon cooling, a system is called a glass if its viscosity exceeds 10^{13} Poise ($10^{12} \text{ Pa} \cdot \text{s}$) [2]. However, this way the transition temperature depends on the cooling rate and measurements are often difficult, especially in soft matter systems. These systems are 'softer' up to a factor of 10^{-12} (2D) or 10^{-15} (3D) which interferes with the idea of a universal, viscosity-dependent definition of T_g . Since glasses, as crystals, are categorized as solids, their mechanical behavior should be characterized by a finite shear modulus μ [3]. A fluid, however, lacks such, at least for low frequencies [4]. Therefore, we expect to see an abrupt change in μ at the onset of vitrification [3, 5, 6]. Although μ is a macroscopic property, in thermal equilibrium it is measurable locally via the equipartition theorem, which makes it applicable to soft matter systems [7, 8].

In this letter, we analyze the elastic properties for both an experimental 2D colloidal glass former and for simulation data of binary hard discs. Our analysis is based on a quasi-equilibrium description of a non-ergodic solid state, which we derive starting from fluid equilibrium upon crossing a kinetic glass transition. The moduli are derived from thermally excited modes in the small wave vector, $\mathbf{q} \rightarrow 0$, limit. A sudden rise in the shear modulus marks the onset of vitrification.

The experimental system consists of a binary mixture of super-paramagnetic polystyrene spheres confined to a flat water-air interface [9]. The species A (diameter $\sigma = 4.5 \mu\text{m}$) and B ($\sigma = 2.8 \mu\text{m}$) have a relative concentration of $\xi = N_B/(N_A + N_B) \approx 45\%$ where N_A and N_B are the number of particles of both species in the field of

view. An external magnetic field H , perpendicular to the interface, lets us control the particle interactions *in situ*. This is expressed by the dimensionless coupling parameter

$$\Gamma = \frac{\mu_0}{4\pi} \cdot \frac{H^2 \cdot (\pi n)^{3/2}}{k_B T} (\xi \cdot \chi_B + (1 - \xi) \cdot \chi_A)^2, \quad (1)$$

which acts as an inverse temperature. n denotes the 2D number density and is computed via Voronoi tessellation. $\chi_{A,B}$ is the susceptibility of species A, B. Video microscopy and digital image analysis provides the position of individual particles as function of time.

Our approach is inspired by the one for 2D crystals [10]. For amorphous solids it requires first an experimentally accessible definition of displacements [6]. We start from a fluid, where a collective mean-squared displacement tensor $\mathbf{C}(\mathbf{q}, t) = \langle \Delta \mathbf{u}_{\mathbf{q}}^*(t) \Delta \mathbf{u}_{\mathbf{q}}(t) \rangle$ follows from time-integrating the velocity field $\Delta \mathbf{u}_{\mathbf{q}}(t) = \int_0^t dt' \mathbf{v}_{\mathbf{q}}(t')$. Its Zwanzig-Mori equation of motion is determined by stress kernels $\mathbf{G}(\mathbf{q}, t)$, which reduce to the time-dependent rheological moduli for $q \rightarrow 0$ [12]. In a nonergodic, glassy state they take finite values at infinite time (index ∞), which are related by $\mathbf{C}_{\infty}(\mathbf{q}) = 2 \frac{k_B T n}{q^2} (\mathbf{G}_{\infty}(\mathbf{q}))^{-1}$. Then, the functions $\hat{\mathbf{C}}(\mathbf{q}, t) = \frac{1}{2} (\mathbf{C}_{\infty}(\mathbf{q}) - \mathbf{C}(\mathbf{q}, t))$, can be argued to have all properties of auto-correlation functions, so that one can write them as $\hat{\mathbf{C}}(\mathbf{q}, t) = \langle \mathbf{u}_{\mathbf{q}}(t)^* \mathbf{u}_{\mathbf{q}} \rangle^{\text{glass}}$, where $\mathbf{u}_{\mathbf{q}}(t)$ is a displacement fluctuation. The superscript 'glass' indicates that averaging is done in a restricted phase space set by the glassy state. As the so obtained displacement fluctuations are ergodic, time and ensemble averages agree. The former shall be denoted by an overbar so that $\bar{\mathbf{r}}_i$ is the average position of particle $i \in [1, N]$ during the time interval Δt . Assuming that the particle displacements $\mathbf{u}_i(t) = \mathbf{r}_i(t) - \bar{\mathbf{r}}_i$ are small, the displacement field in an amorphous solid follows [12]:

$$\mathbf{u}_{\mathbf{q}}(t) = \frac{1}{\sqrt{N}} \sum_{i=1}^N e^{i\mathbf{q} \cdot \bar{\mathbf{r}}_i} \mathbf{u}_i(t) \quad (2)$$

It differs from earlier proposals [13], where coarse-grained fields were considered. This completes our derivation that the equal-time average of the squared displacements is given by elastic coefficients, which are frozen-in contributions in q -dependent stress kernels. The expression for \bar{r}_i holds as long as Δt is smaller than the relaxation time τ_α which was extracted from the mean square displacement of the particle coordinates for high values of Γ . Given that in these states the mean square displacement does not exceed 1/100 of the particles radii within $10^4 s$, we are confident that dynamical arrest is experimentally achieved on this timescale [14, 15].

The Eigenvalues λ_s (the subscript s denotes polarization) of the dynamical matrix $D_{\mu\nu}$ are the spring constants of our system, and can thus be computed from:

$$\frac{1}{\langle |u_s(\mathbf{q})|^2 \rangle^{\text{glass}}} = \frac{\lambda_s}{k_B T}, \quad (3)$$

We call the $\lambda_s(\mathbf{q})$ 'dispersion relation' using quotation marks, keeping in mind that the motion is over-damped due to the surrounding solvent. By applying this method, we implicitly assume only that the system is homogeneous and isotropic corresponding to continuum elasticity theory. In atomic and molecular glasses, recent

progress has shown that vibrational modes undergo a crossover from propagation to localization due to diffraction upon decreasing the wavelength when the local structure of the material can not be ignored any more [16–18], which may be connected to the 'boson peak' (AOP) [19, 20]. In recent colloidal work [21–23], the density of states (DOS) was studied and the associated modes showed 'swirling motions'. In our approach, DOS and AOP can be studied as functions of frequency [24].

In Fig. 1 we present the computed 'dispersion relation' for different interaction parameters. Filled and empty symbols represent spring constants for longitudinal and transverse waves, respectively. The growing amplitude of the curves for increasing Γ reflects the expected stiffening of the system upon cooling. The black vertical line marks the 'Brillouin Zone' edge. Unlike a crystal, a disordered (isotropic) system exhibits no symmetry points in reciprocal space. Therefore, we define the 'Brillouin Zone' simply as a circle with diameter $2\pi/a$, where a denotes the average inter-particle distance. Accordingly, our measured 'dispersion relations' are not sensitive to the direction of \mathbf{q} , which we confirmed by rotating our field of view. In a crystal, the 'dispersion relation' scales with the coupling parameter since the spring constants are linear in Γ [10]. Interestingly, we do not find this scaling with Γ in the amorphous solid [12]. This hints towards a subtle change in structure since particle distances affect the dipolar particle repulsion.

In high symmetry crystals in 2D and amorphous solids, the elasticity tensor $C_{\mu\nu\sigma\tau}$ possesses only two independent elements. These two elements can be expressed via the Lamé coefficients μ and λ of continuum elasticity theory. Following the method described in [7], we extract the Lamé coefficients from the 'dispersion relation' as

$$\frac{a^2(2\mu + \lambda)}{k_B T} = \lim_{\mathbf{q} \rightarrow \mathbf{0}} [q^2 \langle |u_{\parallel}(\mathbf{q})|^2 \rangle^{\text{glass}}]^{-1}, \quad (4)$$

$$\frac{a^2 \mu}{k_B T} = \lim_{\mathbf{q} \rightarrow \mathbf{0}} [q^2 \langle |u_{\perp}(\mathbf{q})|^2 \rangle^{\text{glass}}]^{-1}. \quad (5)$$

We chose an intermediate regime ($0.8 < qa < 2.0$) for the extrapolation $\mathbf{q} \rightarrow \mathbf{0}$ where the data for linear regression fits best [7, 11]. In two dimensions, μ gives the shear modulus and $\mu + \lambda$ the bulk modulus. As we extract the elastic constants for $\mathbf{q} \rightarrow \mathbf{0}$, we are only accounting for long wavelength modes in elastic continuum theory.

Next, we validate our method by studying finite time and size effects, i.e. the frequency and window size dependence of $\mu(\omega)$. It is known that for high frequencies, even fluids exhibit a nonzero shear modulus [4]. We therefore reduce the time interval Δt for which averaged positions are computed. This results in an increased probing frequency. Fig. 2 clearly indicates the expected growth of the shear modulus μ for shorter Δt for

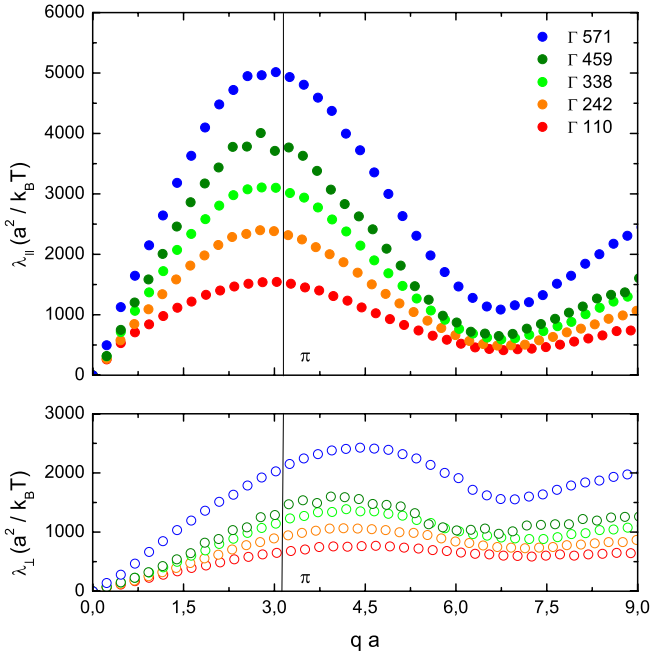


FIG. 1. The 'dispersion relation' for different effective temperatures as extracted from the displacements of particles from their equilibrium position. Filled and empty symbols represent longitudinal and transverse waves, respectively. The black vertical line marks the edge of the 'Brillouin Zone' which we define as a circle in q space with diameter $2\pi/a$ (a being the next neighbor distance).

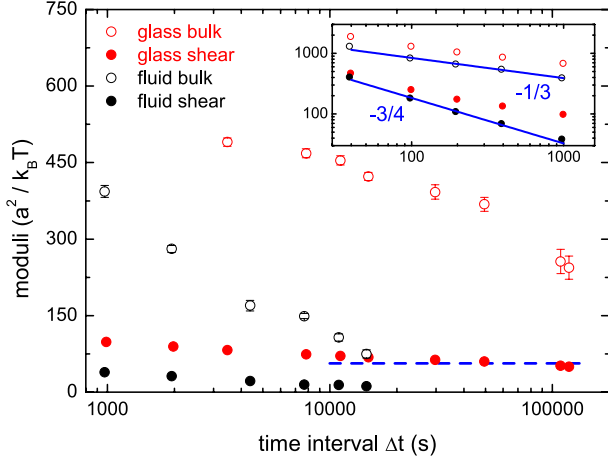


FIG. 2. For high frequencies $\omega \propto 1/\Delta t$ (short trajectories), the expected increase in the shear modulus μ (filled circles) is observed. On long timescales, the shear modulus does not change in the glass (blue dashed line gives best fit) whereas it decays for the fluid. For the bulk modulus (empty circles), however, we observe a significant decrease upon reaching the relaxation time regime. The inset shows a log-log representation of the high frequency region where we find a power law behavior.

both liquids ($\Gamma = 169$) and amorphous solids ($\Gamma = 394$). These results are consistent with [3]. At the same time, we see that for low probing frequencies, the exact value of Δt makes no significant difference for computing the shear modulus. This is marked by a plateau of the shear modulus in the time domain ranging to values beyond the plateau in the mean square displacements where α -relaxations are already visible but the intermediate scattering function did not decay yet to $1/e$ ($\Delta t < \tau_\alpha$). The plateau value of the shear modulus ranges from 10^4 s up to more than 10^5 s (which is the longest sampling time). Hence, Δt is set to ≈ 14400 s for all studied Γ .

The bulk modulus of the glassy system shows another interesting feature on long timescales (Fig. 2, empty red circles). The onset of the observed decay for low frequencies or long trajectories (10^5 s) roughly coincides with the onset of the relaxation time τ_α . Structural relaxation affects longitudinal modes because their amplitudes are extremely small. Transversal modes, however, have about 10 times larger amplitudes. Therefore the decay of the bulk modulus might indicate structural relaxation processes in the α -regime or Mermin-Wagner fluctuations [25] known from 2D crystals. The inset of Fig. 2 shows the high frequency behavior of bulk and shear modulus. We find a power law dependence for almost two decades. The blue lines are guides to the eye with exponents of $-3/4$ and $-1/3$.

Furthermore, we examine finite size effects for the system at $\Gamma = 458$ in Fig. 3 (a). By varying the

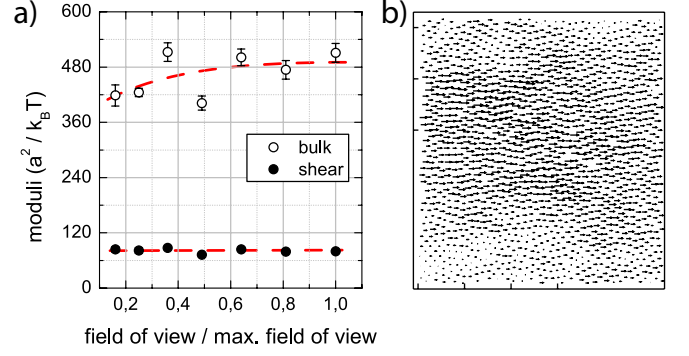


FIG. 3. (a) Effect of a reduced field of view on the elastic properties. The red dashed lines are guides to the eye. (b) Low frequency (long wavelength) mode acquired by diagonalisation of the displacement covariance matrix. The expected plane wave character is found.

window size A/A_0 , we reduce the maximum resolvable wavelength. A significant change in the extracted bulk moduli appears at $\approx 50\%$ of the largest field of view ($A_0 = 589 \mu m^2$). This is illustrated by the red dashed line. To a smaller extent, this feature can also be found in the shear modulus. To check the nature of the long wavelength excitations, the method described in [21–23] was used. An eigenvector of the $2N \times 2N$ covariance matrix $C_{ij} = \langle u_i(t)u_j(t) \rangle$ visualises the displacement field of a mode with a frequency given by the corresponding eigenvalue. Decomposition of the field into the x component for a low frequency mode is shown in Fig. 3 (b). The large coherent motion of this proves the expected plane wave character.

The resulting moduli are shown in Fig. 4. As expected, the shear modulus μ is zero in the fluid phase (first three data points). As we further cool down our sample, we find an onset of μ , indicating the beginning of vitrification in which the system becomes rigid (indicated by the shading). Its magnitude compares well to a mode coupling calculation $\mu = 13nk_B T$ for this system at the glass transition [26]. In order to address the question [6], whether the shear modulus jumps to a finite value at the glass transition or grows continuously from zero in the fluid, we performed Brownian dynamics simulations of a binary mixture of hard discs in two dimensions [12, 27]. Figure 5 shows data for μ evaluated according to Eq. (5) for different time windows Δt . The density range spans the mode coupling glass transition at $\phi_c \approx 0.796$ [27]. The modulus takes finite values as long as the structural relaxation time τ_α exceeds Δt . Approaching the glass transition from above, μ softens but stays finite, while on the fluid side, it vanishes, $\mu = 0$ for $\Delta t > \tau_\alpha$. The inset of Fig. 5 shows that μ agrees with the long time limit of the shear modulus $G_\infty = G(t \rightarrow \infty)$, supporting

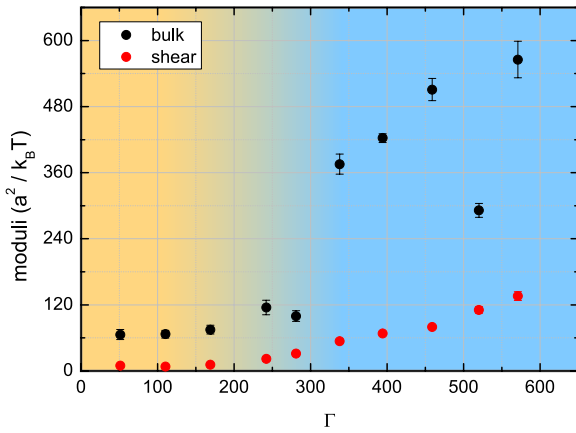


FIG. 4. At $\Gamma \approx 200$, we find an onset of the shear modulus (red circles). This marks the temperature where the system starts to undergo vitrification. Cooling the system below T_g , growing spring constants lead to an increase in stiffness. Shading indicates the crossover from fluid (yellow) to glass (blue).

our analysis.

In conclusion, we have shown that video microscopy allows us to study the spatially Fourier-transformed displacement field of an amorphous solid. We derived its quasi-equilibrium average which, generalizing the classical equipartition theorem, is connected to the thermal energy and stress correlations. In the long wavelength limit we extracted the bulk and shear modulus of the system. The discontinuous onset of a finite quasi-equilibrium shear modulus separates the fluid phase from the amorphous solid.

P.K. gratefully acknowledge financial support of the Young Scholar Fund, University of Konstanz.

-
- [1] P. G. Debenedetti and F. H. Stillinger, *Nature* **410**, 259 (2001).
 - [2] C. A. Angell, *J. Non-Cryst. Solids* **102**, 205 (1988).
 - [3] Y. H. Jeong, *Phys. Rev. A* **36**, 766 (1987).
 - [4] R. A. Apakshv and V. V. Pavlov, *Fluid Dynamics* **32**, 1 (1997).
 - [5] J.-L. Barrat, J.-N. Roux, J.-P. Hansen, and M. L. Klein, *Europhys. Lett.* **7**, 707 (1988).
 - [6] G. Szamel and E. Flenner, *Phys. Rev. Lett.* **107**, 105505 (2011).
 - [7] H. H. von Grünberg, P. Keim, K. Zahn, and G. Maret, *Phys. Rev. Lett.* **93**, 255703 (2004).
 - [8] D. Reinke, H. Stark, H. H. von Grünberg, A. B. Schofield, G. Maret, and U. Gasser, *Phys. Rev. Lett.* **98**, 038301 (2007).
 - [9] F. Ebert, P. Dillmann, G. Maret, and P. Keim, *Rev. Sci. Instr.* **80**, 083902 (2009).

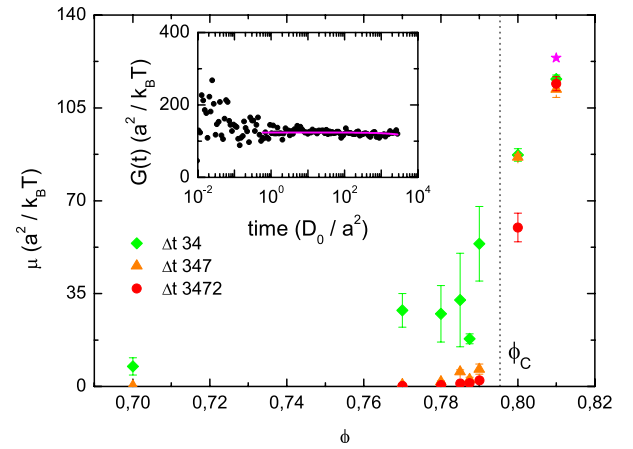


FIG. 5. Shear moduli μ from simulations of a glassy mixture as function of area fraction ϕ . With increasing trajectory length (given in units of D_0/a^2), μ in the fluid converges towards zero. Crossing ϕ_c , μ jumps to a finite value for $\Delta t < \tau_\alpha$. Inset: Time dependent shear modulus $G(t)$ at $\phi = 0.81$ calculated from the stress-stress autocorrelation function [12]. Its plateau value $G_\infty = 124$ (magenta horizontal line is given as star in the main figure) agrees within statistical error with the value of $\mu = 114$ from Eq. (5).

- [10] P. Keim, G. Maret, U. Herz, and H. H. von Grünberg, *Phys. Rev. Lett.* **92**, 215504 (2004).
- [11] The error bars in Fig. 2 - Fig. 5 stem from the linear regression of the extrapolation $q \rightarrow 0$ (see also inset of Fig. 2, supp. mat.).
- [12] Supplementary material
- [13] I. Goldhirsch and C. Goldenberg, *Eur. Phys. J. E* **9**, 245 (2002).
- [14] S. Mazoyer, F. Ebert, G. Maret, and P. Keim, *Euro. Phys. Lett.* **88**, 66004 (2009).
- [15] H. König, R. Hund, K. Zahn, and G. Maret, *Euro. Phys. Jour. E* **18**, 287 (2005).
- [16] B. Rufflé, M. Foret, E. Courtens, R. Vacher, and G. Monaco, *Phys. Rev. Lett.* **90**, 095502 (2003).
- [17] P. B. Allen, J. L. Feldman, J. Fabian, and F. Wooten, *Phil. Mag. B* **79**, 1715 (1999).
- [18] J. Hafner, *J. Phys. C: Solid State Phys.* **16**, 5773 (1983).
- [19] F. Léonforte, *J. Non-Cryst. Solids* **357**, 552 (2011).
- [20] F. Léonforte, A. Tanguy, J. P. Wittmer, and J.-L. Barrat, *Phys. Rev. Lett.* **97**, 055501 (2006).
- [21] A. Ghosh, V. K. Chikkadi, P. Schall, J. Kurchan, and D. Bonn, *Phys. Rev. Lett.* **104**, 248305 (2010).
- [22] D. Kaya, N. L. Green, C. E. Maloney, and M. F. Islam, *Science* **329**, 329 (2010).
- [23] K. Chen, W. G. Ellenbroek, Z. Zhang, D. T. N. Chen, P. J. Yunker, S. Henkes, C. Brito, O. Dauchot, W. van Saarloos, A. J. Liu, and A. G. Yodh, *Phys. Rev. Lett.* **105**, 025501 (2010).
- [24] W. Götze and M. R. Mayr, *Phys. Rev. E* **61**, 587 (2000).
- [25] N. D. Mermin, *Phys. Rev.* **176**, 250 (1968).
- [26] R. Seyboldt, D. Hajnal, F. Weysser, and M. Fuchs, submitted to *Soft Matter* (2011).
- [27] F. Weysser and D. Hajnal, *Phys. Rev. E* **83**, 041503 (2011).

Elastic Properties of 2D amorphous solids: Supplementary material

(Dated: November 9, 2011)

This supplementary material contains technical details of the theoretical approach (part I) and additional simulation results (part II) supporting the conclusions in the main text. Part III contains additional experimental information.

I: DISPLACEMENTS IN GLASS

In order to define the displacement field in glass, we assume the existence of a kinetic glass transition between ergodic fluid and nonergodic glass states, and start from the ergodic fluid side. Here fluctuations around the equilibrium values decorrelate at long times. Crossing the glass transition, the states become nonergodic. Fluctuations (of even time-parity) can not decorrelate and the frozen-in correlations describe the glassy state. To prepare the grounds for capturing local correlations, we refrain from coarse-graining [13].

Basic equations

In a fluid, we consider the velocity autocorrelation tensor, $\mathbf{K}(\mathbf{q}, t) = \langle \mathbf{v}_{\mathbf{q}}^*(t) \mathbf{v}_{\mathbf{q}}(0) \rangle$, where for N point-particles $\mathbf{v}_{\mathbf{q}}(t) = (1/\sqrt{N}) \sum_{i=1}^N e^{i\mathbf{q} \cdot \mathbf{r}_i(t)} \dot{\mathbf{r}}_i(t)$. Its initial value is $\mathbf{K}(\mathbf{q}, 0) = \frac{k_B T}{m} \mathbf{1}$. Equilibrium averaging is done with the Gibbs-Boltzmann distribution. Time dependence in classical Newtonian systems is given by the Liouville operator \mathcal{L} , which describes the time derivative $\mathcal{L} = -i\partial_t$. In an isotropic system, the tensor of velocity correlation functions splits into a longitudinal (connected to the compressional) and a transverse velocity correlator; in two dimensions and with \mathbf{q} in x -direction: $K^{\parallel}(q, t) = K_{xx}(q, t) = \langle v_x(q\hat{\mathbf{x}}, t)^* v_x(q\hat{\mathbf{x}}, 0) \rangle$ and $K^{\perp}(q, t) = K_{yy}(q, t) = \langle v_y(q\hat{\mathbf{x}}, t)^* v_y(q\hat{\mathbf{x}}, 0) \rangle$; off-diagonal elements vanish. Similar decompositions hold for all following tensors because of isotropy.

The definition of displacement differences which we suggest uses the velocity field:

$$\Delta \mathbf{u}_{\mathbf{q}}(t) = \int_0^t dt' \mathbf{v}_{\mathbf{q}}(t'). \quad (6)$$

Because these displacement differences vanish for short times and become arbitrarily large in a fluid at long times, a well defined quantity is the tensor of collective mean-squared displacements:

$$\mathbf{C}(\mathbf{q}, t) = \langle \Delta \mathbf{u}_{\mathbf{q}}^*(t) \Delta \mathbf{u}_{\mathbf{q}}(t) \rangle = 2 \int_0^t dt' (t-t') \mathbf{K}(\mathbf{q}, t'), \quad (7)$$

where stationarity is used to simplify the two time integrations to one.

Equations of motion

In order to find the displacement correlations at long times in a nonergodic state (glass), the familiar equations of motion of the velocity correlation functions are used [28]. Newton's equation $i\mathcal{L}\dot{\mathbf{r}}_i(t) = \partial_t^2 \mathbf{r}_i(t) = \mathbf{F}_i(t)/m$ enters, where \mathbf{F}_i is the (total) force acting on particle i . This leads to the appearance of a memory kernel $\mathbf{M}(\mathbf{q}, t) = \langle \mathbf{F}_{\mathbf{q}}^* U_{\mathcal{Q}}(t) \mathbf{F}_{\mathbf{q}} \rangle / (mk_B T)$ built with the force fluctuation $\mathbf{F}_{\mathbf{q}} = (1/\sqrt{N}) \mathcal{Q} \sum_i \mathbf{F}_i e^{i\mathbf{q} \cdot \mathbf{r}_i}$. The projector $\mathcal{Q} = 1 - \mathcal{P}$ decouples the fluctuations from the conserved hydrodynamic ones, density and momentum: $\mathcal{P} = \delta \varrho_{\mathbf{q}} \frac{1}{S_q} \langle \delta \varrho_{\mathbf{q}}^* + \mathbf{v}_{\mathbf{q}} \rangle \frac{m}{k_B T} \langle \mathbf{v}_{\mathbf{q}}^* \rangle$, as the reduced resolvent obeys $\partial_t U_{\mathcal{Q}}(t) = -i(\mathcal{Q}\mathcal{L}\mathcal{Q}) U_{\mathcal{Q}}(t)$. \mathcal{Q} also eliminates the kinetic part using that velocities are distributed according to a Maxwellian.

Above equations started from Newtonian dynamics and thus apply on times scales much shorter than the ones of interest in colloids. Coarse graining to obtain equations appropriate for colloids starts from decomposing the forces \mathbf{F}_i on the particles into forces from the solvent $\mathbf{F}_i^{\text{solv}}$ and interparticle forces $\mathbf{F}_i^{\text{pot}}$. The latter arise from a potential $\mathbf{F}_i^{\text{pot}} = -\partial_{\mathbf{r}_i} U$. We assume that solvent and particle forces decouple and that the solvent forces are Markovian and can be captured by a friction coefficient: $\mathbf{M}(\mathbf{q}, t) = \frac{2\zeta}{m} \delta(t) \mathbf{1} + \frac{q^2}{mn} \mathbf{G}_{\mathbf{q}}(t)$. A prefactor q^2 could be pulled in front of the generalized q -dependent modulus (a stress tensor autocorrelation function with reduced resolvent) because of Newton's actio-reactio principle $\sum_i \mathbf{F}_i^{\text{pot}} = 0$. Its elements are defined by

$$\mathbf{G}_{\mathbf{q}}(t) = \frac{n}{k_B T} \left\langle \left(\frac{i}{q} \mathbf{F}_{\mathbf{q}}^{\text{pot}} \right)^* U_{\mathcal{Q}}(t) \left(\frac{i}{q} \mathbf{F}_{\mathbf{q}}^{\text{pot}} \right) \right\rangle, \quad (8a)$$

and for vanishing wavevector become the (potential) moduli:

$$\mathbf{G}(t) = \lim_{q \rightarrow 0} \mathbf{G}_{\mathbf{q}}(t) = \frac{n}{k_B T} \langle (\hat{\mathbf{q}} \cdot \boldsymbol{\sigma}(t)^*) (\boldsymbol{\sigma} \cdot \hat{\mathbf{q}}) \rangle, \quad (8b)$$

where the microscopic stress tensor element

$$\boldsymbol{\sigma} = -\frac{\mathcal{Q}}{\sqrt{N}} \sum_{i=1}^N \mathbf{F}_i \mathbf{r}_i, \quad (8c)$$

and the reduced dynamics simplifies to the full one. Neglecting the inertial term, the overdamped equations of motion of the strain correlators follow:

$$\mathbf{C}(\mathbf{q}, t) + \frac{D_0 q^2}{k_B T n} \int_0^t dt' \tilde{\mathbf{G}}(\mathbf{q}, t-t') \mathbf{C}(\mathbf{q}, t') = 2D_0 t \mathbf{1}, \quad (9)$$

with the short time diffusion coefficient $D_0 = k_B T / \zeta$. To simplify the notation, the (wavevector-dependent) isothermal compressibility of the fluid, $\kappa_q^T = S_q / (k_B T n)$, which entered via density conservation, is included in the moduli with tilde, $\tilde{\mathbf{G}}(\mathbf{q}, t) = \mathbf{G}(\mathbf{q}, t) + (1/\kappa_q^T) \hat{\mathbf{q}} \hat{\mathbf{q}}$.

Phenomenology of glass

In an nonergodic state the time dependent moduli take finite values at infinite time:

$$\tilde{\mathbf{G}}(\mathbf{q}, t \rightarrow \infty) \rightarrow \mathbf{G}_\infty(\mathbf{q}), \quad (10)$$

which predicts from Eq. (9)

$$\mathbf{C}(\mathbf{q}, t \rightarrow \infty) \rightarrow \mathbf{C}_\infty(\mathbf{q}) = 2 \frac{k_B T n}{q^2} (\mathbf{G}_\infty(\mathbf{q}))^{-1}. \quad (11)$$

Displacement fluctuations stay below a finite limit for all times. This nonergodic state is a solid one.

In the glassy state, the relaxation onto the frozen-in components can be studied. Experimentally, this requires the observed state to be deep in the glass in order that the structural relaxation is much slower.

In glass, a displacement fluctuation function $\hat{\mathbf{C}}(\mathbf{q}, t)$ shall be defined as:

$$\hat{\mathbf{C}}(\mathbf{q}, t) = \frac{1}{2} (\mathbf{C}_\infty(\mathbf{q}) - \mathbf{C}(\mathbf{q}, t)). \quad (12)$$

Obviously, it satisfies: $\hat{\mathbf{C}}(\mathbf{q}, t \rightarrow \infty) = \mathbf{0}$, and is bounded by its initial value: $\hat{\mathbf{C}}(\mathbf{q}, t = 0) = \frac{1}{2} \mathbf{C}_\infty(\mathbf{q})$. Anticipating that one can proof that the $\hat{\mathbf{C}}(\mathbf{q}, t)$ are (auto-) correlation functions, one thus concludes that they are ergodic. By definition, they are stationary. We will assume that all familiar relations from ergodicity theory hold [29]. Displacements in the glass are finite and follow from Eq. (6):

$$\Delta \mathbf{u}_\mathbf{q}(t) = \mathbf{u}_\mathbf{q}(t) - \mathbf{u}_\mathbf{q} = (e^{i\mathcal{L}t} - 1) \mathbf{u}_\mathbf{q} \quad (13)$$

The $\hat{\mathbf{C}}(\mathbf{q}, t)$ can then be written as:

$$\hat{\mathbf{C}}(\mathbf{q}, t) = \langle \delta \mathbf{u}_\mathbf{q}(t)^* \delta \mathbf{u}_\mathbf{q} \rangle^{\text{glass}}, \quad (14)$$

where the superscript 'glass' at the bracket indicates that averaging is done in a restricted phase space set by the nonergodic glassy state. The displacement fluctuation is given by: $\delta \mathbf{u}_\mathbf{q}(t) = \mathbf{u}_\mathbf{q}(t) - \langle \mathbf{u}_\mathbf{q} \rangle^{\text{glass}}$, where $\langle \mathbf{u}_\mathbf{q} \rangle^{\text{glass}} = \sqrt{\langle |\mathbf{u}_\mathbf{q}|^2 \rangle^{\text{glass}} - \frac{1}{2} \mathbf{C}_\infty(\mathbf{q})}$.

Discussion

The interpretation of the displacement $\mathbf{u}_\mathbf{q}(t)$ given in Eq. (13) remains to be discussed and how to measure

$\hat{\mathbf{C}}(\mathbf{q}, t)$ experimentally in e.g. a colloidal glass. As displacement fluctuations are ergodic, time and ensemble averages agree. Let $\bar{\mathbf{r}}_i$ be the temporally averaged position of particle i . From Eq. (13) follows assuming that the particle displacements $\mathbf{u}_i(t) = \mathbf{r}_i(t) - \bar{\mathbf{r}}_i$ are small:

$$\begin{aligned} \mathbf{u}_\mathbf{q}(t) - \mathbf{u}_\mathbf{q} &= \int_0^t dt' \sum_{i=1}^N \dot{\mathbf{r}}_i(t') e^{i\mathbf{q} \cdot \bar{\mathbf{r}}_i} (1 + \mathcal{O}(\mathbf{q} \cdot \mathbf{u}_i)) \\ &= \sum_{i=1}^N e^{i\mathbf{q} \cdot \bar{\mathbf{r}}_i} (\mathbf{u}_i(t) - \mathbf{u}_i(0)), \end{aligned} \quad (15)$$

neglecting terms $\mathcal{O}(\mathbf{q} \cdot \mathbf{u}_i)$. Within the first Brillouin zone this holds as long as displacements are much smaller than the average particle separation. Equation (15) leads to Eq. (2) in the letter. In this approximation, $\langle \mathbf{u}_\mathbf{q}(t) \rangle^{\text{glass}} = 0$, and the δ -sign for a fluctuation can be dropped in Eq. (14). From Eqs. (11,12) follows

$$\langle \mathbf{u}_\mathbf{q}^* \mathbf{u}_\mathbf{q} \rangle^{\text{glass}} = \frac{k_B T n}{q^2} (\mathbf{G}_\infty(\mathbf{q}))^{-1}, \quad (16)$$

that the equal-time average of the squared displacements is given by the inverse of the matrix of elastic constants which are the nonergodic contributions in the stress memory functions. This central result, used and tested in the letter, arises from our definition of displacements in glass, which differs from the one presented by Goldhirsch and Goldenberg [13], where $\mathbf{u}_i(t = 0) = 0$ holds and the equal-time average vanishes in linear response.

II: SIMULATION

We simulated a binary mixture of hard discs undergoing Brownian motion using the algorithm proposed by Scala et al. [31]. The system is made up of $N = 1000$ particles, with a diameter ratio of small to big disks $d_s/d_b = 0.7$ and equal number concentrations $x_s = x_b = 1/2$ at a total packing fraction of $\varphi = \frac{\pi N}{4V} (x_s d_s^2 + d_b^2 x_b)$. A detailed analysis of the structural relaxation close to its glass transition can be found in Ref. [27].

The dispersion relations and elastic moduli were obtained as explained in the letter from 10^4 equally spaced snap-shots along one equilibrated simulation trajectory for times up to Δt . Following the method of Alder et al. [30] we also determined the integrated time dependent shear modulus

$$\eta_{xy}(t) = \frac{1}{2k_B T V} \frac{d}{dt} \left\langle \left(\sum_{\text{coll} \in [0;t]} \Delta r_{ij}^y(t_c) \Delta p_{ij}^x(t_c) \right)^2 \right\rangle. \quad (17)$$

Here the sum runs over all collisions up to time t and $\Delta \mathbf{r}_{ij}(t_c)$ denotes the relative distance and $\Delta \mathbf{p}_{ij}(t_c)$ the momentum transfer of two particles at the collision at

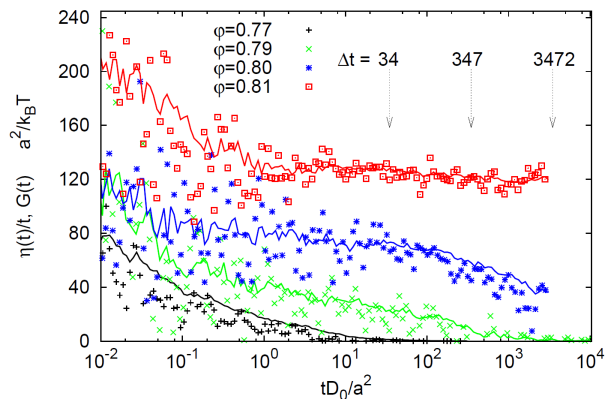


FIG. 6. Shear modulus $G(t)$ (symbols) and $\eta_{xy}(t)/t$ (solid lines) for different packing fractions as depicted in the legend. Arrows indicate the length of the trajectories, used to calculate the values in Fig. 5.

time t_c [32]. The brackets $\langle \dots \rangle$ denote the average over different simulation runs. The integrated shear modulus was determined for 600 independent, equilibrated initial configurations at $\varphi = 0.81$ and for 150 for all other packing fractions. Equilibration was assumed when the correlation functions became independent on the waiting time. The differentiation in Eq. (17) was done numerically, as was the second one to obtain $G(t)$ from $\eta_{xy}(t) = \int_0^t dt' G(t')$. Finally, a three point running average was performed on the data for $G(t)$.

Figure 6 shows $G(t)$ and the integrated shear modulus $\eta_{xy}(t)$ divided by t , which is a good indicator of a plateau $G(t \rightarrow \infty) = G_\infty$. Arrows indicate the lengths of the different trajectories used in the letter to calculate the shear modulus from the average displacement fluctuations; the results are shown in Fig. 5 there. Note that the time-scale in Fig. 6 is logarithmic: Because of the equidistant sampling used to measure $\langle |\mathbf{u}(\mathbf{q})|^2 \rangle$, the final part of the time signal dominates. This explains that for $\varphi = 0.80$ the measurement using $\Delta t = 3472$ is below the shorter ones. The final α -process already affects this measurement.

III: EXPERIMENT

Fig. 7 shows the data of Fig. 1 but normalized with the dimensionless interaction strength Γ . The red circles are in the fluid phase while other colors refer to the amorphous solid state. They do not collapse to a single master curve which hints towards a subtle

change in structure since particle distances affect the dipolar particle repulsion. This change in structure does not affect the 2D density n and is barely visible in the structure factor. Nevertheless, with increasing coupling parameter, particles tend to maximize their pair-distances and the wave vector dependent spring constant λ does not scale linearly with Γ .

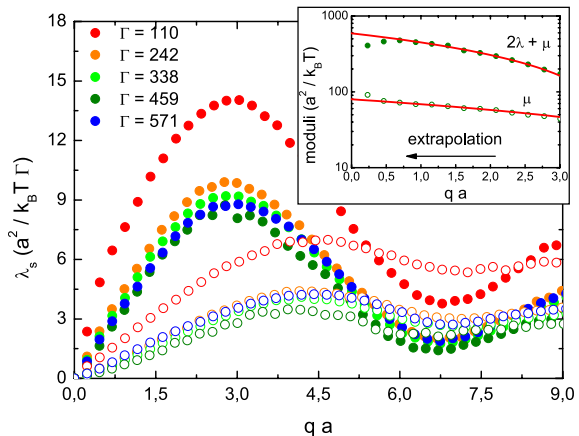


FIG. 7. The normalized 'dispersion relations' for different effective temperatures in the solid state do not collapse to a single curve. The inset shows the extrapolation of the elastic constants from the dispersion relation for $q \rightarrow 0$ at $\Gamma = 459$.

REFERENCES

- [13] I. Goldhirsch and C. Goldenberg, Eur. Phys. J. E **9**, 245 (2002).
- [27] F. Weysser and D. Hajnal, Phys. Rev. E **83**, 041503, (2011)
- [28] Götze, W., in *Liquids, Freezing and Glass Transition*, edited by J. P. Hansen, D. Levesque, and J. Zinn-Justin, Session LI (1989) of Les Houches Summer Schools of Theoretical Physics, (North-Holland, Amsterdam, 1991), 287.
- [29] R. Kubo, J. Phys. Soc. Jpn. **12**, 570 (1957).
- [30] B. J. Alder, D. M. Gass, and T. E. Wainwright, J. Chem. Phys. **53**, 3813 (1970).
- [31] A. Scala, T. Voigtmann, and C. De Michele, J. Chem. Phys. **126**, 134109 (2007).
- [32] O. Henrich, F. Weysser, M. E. Cates, and M. Fuchs, Philos. Trans. R. Soc. A **367**, 5033 (2009).